Received: 2 February 2018 | Revised: 21 June 2018 | Accepted: 26 June 2018

DOI: 10.1002/ajpa.23684

WILEY American Journal of PHYSICAL ANTHROPOLOGY

RESEARCH ARTICLE

Low temperature decreases bone mass in mice: Implications for humans

Amy Robbins | Christina A. T. M. B. Tom | Miranda N. Cosman | Cleo Moursi | Lillian Shipp | Taylor M. Spencer | Timothy Brash | Maureen J. Devlin

Department of Anthropology, University of Michigan, Ann Arbor, Michigan

Correspondence
Maureen J. Devlin, PhD, University of Michigan, 101 West Hall, 1085 S. University Avenue, Ann Arbor, MI 48109.
Email: mjdevlin@umich.edu

Funding information
National Institute of Arthritis and Musculoskeletal and Skin Diseases, Grant/Award Number: P30 AR069620; National Science Foundation, Grant/Award Number: BCS-1638553

Abstract

Objectives: Humans exhibit significant ecogeographic variation in bone size and shape. However, it is unclear how significantly environmental temperature influences cortical and trabecular bone, making it difficult to recognize adaptation versus acclimatization in past populations. There is some evidence that cold-induced bone loss results from sympathetic nervous system activation and can be reduced by nonshivering thermogenesis (NST) via uncoupling protein (UCP1) in brown adipose tissue (BAT). Here we test two hypotheses: (1) low temperature induces impaired cortical and trabecular bone acquisition and (2) UCP1, a marker of NST in BAT, increases in proportion to degree of low-temperature exposure.

Methods: We housed wildtype C57BL/6J male mice in pairs at 26 °C (thermoneutrality), 22 °C (standard), and 20 °C (cool) from 3 weeks to 6 or 12 weeks of age with access to food and water ad libitum (N = 8/group).

Results: Cool housed mice ate more but had lower body fat at 20 °C versus 26 °C. Mice at 20 °C had markedly lower distal femur trabecular bone volume fraction, thickness, and connectivity density and lower midshaft femur cortical bone area fraction versus mice at 26 °C ($p < .05$ for all). UCP1 expression in BAT was inversely related to temperature.

Discussion: These results support the hypothesis that low temperature was detrimental to bone mass acquisition. Nonshivering thermogenesis in brown adipose tissue increased in proportion to low-temperature exposure but was insufficient to prevent bone loss. These data show that chronic exposure to low temperature impairs bone architecture, suggesting climate may contribute to phenotypic variation in humans and other hominins.

KEYWORDS

nonshivering thermogenesis, sympathetic tone, temperature, trabecular bone

1 | INTRODUCTION

Hominin skeletal phenotype varies geographically, such that populations at high latitudes tend to have broader, more massive bodies with shorter distal limb segments compared to populations at lower latitudes (Churchill, 1998; Foster & Collard, 2013; Holliday, 1997; Holliday & Hilton, 2010; Katzmarzyk & Leonard, 1998; Pearson, 2000; Ruff, 1994, 2002). According to Bergmann's Law and Allen's Rule, these shape differences increase fitness in cold climates by lowering surface area:volume ratio and decreasing heat loss (Allen, 1877; Bergmann, 1847; Ruff, 1993). However, the extent to which these patterns reflect genetic adaptation versus developmental plasticity during growth is largely unknown. It is also unclear whether temperature directly influences human variation in aspects of skeletal phenotype such as cortical bone cross-sectional geometry or trabecular bone microarchitecture.

Several recent observations suggest the skeleton may have developmentally plastic responses to temperature. First, the well-known historical positive correlations of latitude with body mass and bi-iliac breadth and negative correlations with surface area/mass ratio and

distal limb segment length (Roberts, 1953; Ruff, 1994) have weakened in recent years (Katzmarzyk & Leonard, 1998). This trend is clearly due in part to secular trends in body mass, but potentially also reflects reduced cold exposure. Second, in retrospective data, cold-adapted populations tend to have more robust bones than heat-adapted populations do, perhaps reflecting their higher body mass (Pearson, 2000). However, other studies of cold-dwelling humans found low cortical thickness and bone mineral density as well as accelerated bone loss with aging, although it is unclear whether these patterns are due to temperature, high fat and protein intake, or both (Harper, Laughlin, & Mazess, 1984; Lazenby, 1997; Leslie et al., 2006; Leslie, Weiler, Lix, & Nyomba, 2008; Mazess & Mather, 1974, 1975; Thompson & Gunness-Hey, 1981; Wallace, Nesbitt, Mongle, Gould, & Grine, 2014). Finally, in animal models, changes in limb bone length can be produced experimentally within a single generation simply by raising mice in cold or warm temperatures (Serrat, King, & Lovejoy, 2008), and increasing housing temperature to mouse thermoneutrality reduces trabecular bone loss (Iwaniec et al., 2016). These provocative studies demonstrate that at least in rodents, bone responds dynamically to temperature, such that the cold-dwelling skeletal phenotype may not be entirely genetically mediated.

If bone exhibits developmentally plastic responses to temperature, then it is essential to understand how interactions between cold stress and thermogenic mechanisms alter skeletal acquisition. In mammals, temperature is primarily maintained by basal metabolic rate, augmented during cold challenge by mechanisms such as shivering and nonshivering thermogenesis (NST). NST occurs in mitochondria-rich adipocytes called brown adipose tissue (BAT) and has recently been the subject of renewed interest. Although the constitutive BAT depots present in human newborns regress after infancy (Heaton, 1972), a type of BAT known as beige fat can be induced in adults in response to cold exposure (Cypess et al., 2009; Saito et al., 2009; Sharp et al., 2012; van Marken Lichtenbelt et al., 2009; Virtanen et al., 2009; Wu et al., 2012). Such active BAT is found after cold challenge in 50%–90% of adults under age 35, but only 8% of adults over 35 (Saito et al., 2009; van Marken Lichtenbelt et al., 2009). BAT is more abundant in winter than in summer, and in outdoor versus indoor workers (Au-Yong, Thorn, Ganatra, Perkins, & Symonds, 2009; Huttunen, Hirvonen, & Kinnula, 1981). This environmental responsiveness suggests that beige fat may have aided hominin expansion to colder regions. High-latitude populations have higher basal metabolic rates than predicted for their lean mass, potentially due in part to nonshivering thermogenesis in BAT (Leonard & Levy, 2015), and it is reasonable to hypothesize that earlier cold-adapted hominins also relied in part on BAT thermogenesis (Steegmann Jr., 2007).

BAT is also a potential mediator of skeletal responses to cold stress (reviewed in Devlin, 2015; Lowell & Spiegelman, 2000). Cold exposure increases sympathetic tone, leading to bone loss via hypothalamic signaling to beta2-adrenergic receptors on osteoblasts. Cold exposure activates uncoupling protein-1 (UCP1) in the inner mitochondrial membrane to divert fatty acid and glucose oxidation to instead generate heat (Nicholls & Rial, 1999), which would increase body temperature and reduce sympathetic tone. In animal models, in the absence of BAT, chronic SNS activation induces bone loss (Kajimura et al., 2011). The *Misty* mouse model of dysfunctional BAT has high sympathetic tone and low bone mass that is mitigated by the beta-adrenergic antagonist propranolol, suggesting that BAT might protect bone mass by buffering the skeleton against SNS-induced bone loss (Motyl et al., 2013). In support of positive skeletal effects of BAT, recent studies in humans report that BAT is positively associated with bone mineral density (BMD) and bone cross-sectional area in subadults and adults of both sexes (Bredella et al., 2012; Bredella, Gill, Rosen, Klibanski, & Torriani, 2014; Lee et al., 2013; Ponrartana et al., 2012).

To delineate the mechanistic relationships between low-temperature, nonshivering thermogenesis in brown adipose tissue, and skeletal acquisition, here we used controlled experiments in mice housed at subthermoneutral temperatures or near thermoneutrality (Gaskill et al., 2012) as a model for exposure to low temperature in humans. Human thermoneutrality ranges from ~26 to 32 °C when unclothed (Erikson, Krog, Andersen, & Scholander, 1956; Hardy & Dubois, 1937; Kingma, Frijns, Schellen, & van Marken Lichtenbelt, 2014) and from ~20 to 25 °C in clothing (Kingma et al., 2014; Kingma, Frijns, & van Marken Lichtenbelt, 2012; Lodhi & Semenkovich, 2009), although individual tolerance depends on factors including body shape, fat mass, and acclimatization. The equivalent thermoneutral temperature in the mouse is a subject of ongoing debate. Laboratory mice are typically housed at 20–22 °C, but recent studies have argued that thermoneutrality for mice is closer to 30 °C and that mice housed at standard temperature are chronically cold stressed (Cannon & Nedergaard, 2011; Gaskill et al., 2012; Gordon, 2012; Karp, 2012; Lodhi & Semenkovich, 2009; Overton, 2010). In contrast, Speakman and Keijer (2012) noted that both humans and mice have energy expenditure of ~1.6–1.8 times basal metabolic rate at 22 °C, such that on a metabolic basis, this temperature is appropriate for mice being used to model humans. However, a more recent study using indirect calorimetry found that energy expenditure in singly housed mice is 1.8 times basal metabolic rate at 30 °C and increases to 3.1 times basal metabolic rate at 22 °C (Fischer, Cannon, & Nedergaard, 2018). Mice at 22 °C also exhibit significantly higher respiratory quotient, glucose uptake and UCP1 activity in BAT (David, Chatziioannou, Taschereau, Wang, & Stout, 2013). These studies show that mice expend increased energy on nonshivering thermogenesis when housed at or below standard vivarium temperature.

Here we compare the effects of housing at temperatures from 20–26 °C to test the following hypotheses: (1) that low temperature reduces skeletal acquisition in young, rapidly growing animals and (2) that UCP1 protein expression as a marker of increased NST in BAT is proportional to the decrease in housing temperature. For hypothesis (1), we predicted that exposure to low temperature during rapid skeletal growth would increase sympathetic tone, leading to weaker trabecular microarchitecture, cortical bone cross-sectional geometry, and bone strength. Given evidence from early studies that cold exposure increases bone marrow adiposity, we predicted that cool housed mice would have more and larger adipocytes in distal femur bone marrow (Huggins & Blocksom, 1936). For hypothesis (2), we predicted that increased UCP1 expression in BAT may partially or completely prevent low temperature-induced bone loss by increasing body temperature and blunting the rise in sympathetic tone. Overall, we predicted that BMD, cortical and trabecular bone parameters, and histological

indices of bone formation would be negatively correlated with low temperature and positively correlated with UCP1 levels as a marker of NST.

2 | MATERIALS AND METHODS

2.1 | Mice and diet intervention

We obtained 3-week-old male C57BL/6J (B6) mice (The Jackson Laboratory, Bar Harbor, ME) and assigned them to housing at 20 °C (low temperature, "cool"), 22 °C (standard housing temperature, "control"), or 26 °C (near thermoneutrality, "warm"), and a normal diet ad libitum (PicoLab 5L0D, LabDiets, St. Louis, MO, 13% kcal/fat, 30% kcal/protein, 57% kcal/carbohydrate) until 6 or 12 weeks of age (N = 8/group).

Baseline body mass and bone mineral density did not differ among groups. Mice were housed in pairs to provide socialization but minimize elevated nest temperatures. Toth, Trammell, and Ilsley-Woods (2015) tested the effect of housing density on cage temperature at 22, 26, and 30 °C and found no significant difference in ambient temperature when density increased from one mouse to two mice per cage. Therefore, to avoid introducing an additional variable by singly housing (Nagy, Krzywanski, Li, Meleth, & Desmond, 2002), we maintained mice at two per cage. Mouse body mass and food intake were measured two to three times weekly on a digital scale. All procedures were approved by the University of Michigan Institutional Animal Care and Use Committee.

2.2 | Peripheral dual-energy X-ray absorptiometry

In vivo assessment of whole-body bone mineral density (BMD, g/cm^2), bone mineral content (BMC, g), and body composition was performed at 3, 6, 9, and 12 weeks of age using peripheral dual-energy X-ray absorptiometry under inhaled isoflurane (pDXA, PIXImus I, GE Lunar Corp.), as previously described (Bouxsein et al., 2005, 2009; Devlin et al., 2016).

2.3 | Euthanasia and specimen harvesting/preparation

At the conclusion of the experiment, mice were sacrificed by CO_2 inhalation. Blood was collected by cardiac puncture to assess indices of bone turnover (Devlin et al., 2014). Epididymal white adipose and interscapular brown adipose depots were dissected, snap frozen in liquid nitrogen, and stored at −80 °C (Murray, Havel, Sniderman, & Cianflone, 2000). Femurs were harvested and cleaned of soft tissue. The right femur was prepared for imaging and biomechanical testing by wrapping in saline soaked gauze, and then stored airtight at −20 °C. The left femur was prepared for histology in 70% ethanol at 4 °C.

2.4 | Histology

Left femora were fixed in 70% ethanol and undecalcified bones were embedded in polymethylmethacrylate (N = 4–5/group). Sagittal sections (4–8 μm thick) were cut with Jung 2065 and 2165 microtomes (Leica Biosystems, Buffalo Grove, IL) and stained with Von Kossa/tetrachrome stain for assessment of marrow adiposity in the distal femoral metaphysis using Bioquant OSTEO software (Bioquant Image Analysis, Nashville, TN). Although marrow lipids are removed during tissue processing, adipocytes remain identifiable as round, unstained spaces (Aguirre et al., 2007). The region of interest included the secondary spongiosa of the distal femur beginning 150 μm proximal to the growth plate and extending proximally 1,200 μm, and mediolaterally across the entire bone section at a margin of 150 μm from the cortical edges. Measurements included the number of adipocytes and the percentage of adipocyte volume per tissue volume. Terminology followed the Histomorphometry Nomenclature Committee of the American Society for Bone and Mineral Research (Dempster et al., 2013).

2.5 | mRNA isolation and quantification

To quantify expression of NST marker UCP1, total RNA was prepared from liquid nitrogen snap-frozen BAT via standard TRIzol extraction (Sigma, St. Louis, MO). RNA was recovered in 30 μL RNase-free water, quantitated on a NanoDrop 2000 spectrophotometer (Thermo Fisher Scientific, Waltham, MA), and treated with Promega RQ1 RNase-free DNase to remove any residual genomic DNA (Promega M6101, Madison, WI). Preparation and generation of cDNA was made with the Promega GoScript Reverse Transcriptase System (Promega A5000, Madison, WI) according to manufacturer's instructions.

Gene expression was measured on a CFX384 Real-Time PCR detection system (Bio-Rad Laboratories, Hercules, CA) at the University of Michigan Molecular Biology Core. Thirty nanograms of cDNA was used per 15 μL PCR reaction with SYBR Green PCR Master Mix (Applied Biosystems, Thermo Fisher Scientific 4309155, Waltham, MA) according to manufacturer's recommendations. All reactions were performed in triplicate. Specific primers (Invitrogen, Carlsbad, CA) were used at 300 nmol per reaction for either target gene UCP1 (F 5′ GGA TGG TGA ACC CGA CAA CT 3′, R 5′ CTT GGA TCT GAA GGC GGA CT 3′) or housekeeping gene cyclophilin (F 5′ CAA ATG CTG GAC CAA ACA CAA 3′). Primer reaction specificity was verified via melting curve analysis and efficiency varied between 101% and 98% for UCP1 and cyclophilin, respectively, when spanning 5 orders of magnitude. UCP1 relative gene expression was determined by the ΔΔ-Ct method (Livak & Schmittgen, 2001).

2.6 | Protein isolation and quantification

To quantify UCP1 expression, total protein was extracted via standard methods in RIPA buffer (Thermo Scientific, Waltham, MA) with protease (Sigma, St. Louis, MO) and phosphatase (Roche, Basel, Switzerland) inhibitors added. Protein concentration was determined via BCA assay (Pierce, Rockford, IL). Western blot followed standard SDS-PAGE procedures using Mini-PROTEAN Tetra Cell (Bio-Rad, Hercules, CA) equipment. After transfer, gel was stained with 0.1% Coomassie G-250 (Thermo Scientific, Waltham, MA) and imaged to visualize total protein loading. Primary antibodies for rabbit anti-UCP1 (Thermo Fisher Scientific #PA1–24894) and mouse anti-GAPDH antibody (Ambion #AM4300, Carlsbad, CA) were used 1:1k and 1:2k,

respectively, in TBST+5% nonfat dry milk. HRP-conjugated secondary antibodies for anti-rabbit and anti-mouse (Thermo Fisher Scientific #65-6120 and #31430, Rockford, IL) were used 1:30,000 in TBST+5% nonfat dry milk, bands visualized by ECL (Advantsa, Menlo Park, CA) and signals captured on a c600 imaging system (Azure Biosystems, Dublin, CA). Bands were quantitated using ImageJ density values, and UCP1 expression determined via total protein normalization (Aldridge, Podrebarac, Greenough, & Weiler, 2008; Gilda & Gomes, 2013).

2.7 | Serum leptin measurement

Terminal blood samples were collected in MiniCollect serum separation tubes (Greiner Bio-One, Kremsumünster, Austria) at time of sacrifice by cardiac puncture, stored on wet ice, and serum isolated by centrifuge. Serum was stored at −80 °C until analysis. Serum leptin was measured in duplicate by ELISA (Crystal Chem, Downers Grove, IL) according to manufacturer's instructions and quantitated on microplate reader (Molecular Devices, Sunnyvale, CA).

2.8 | Mouse trabecular and cortical bone morphology by microCT

Assessment of bone morphology and microarchitecture was performed with high-resolution microcomputed tomography (eXplore Locus SP, GE Healthcare, Chalfont, UK) using scan parameters of 80 kVP, 0.45 mA. In brief, the metaphysis of the distal femur was scanned using an 18 μm isotropic voxel size. Images were reconstructed, filtered, and thresholded using a specimen-specific threshold (Meinel et al., 2005; Ridler & Calvard, 1978). Morphometric parameters were computed using a direct 3D approach that does not rely on any assumptions about the underlying structure (Hildebrand, Laib, Muller, Dequeker, & Ruegsegger, 1999; Hildebrand & Rüegsegger, 1997). Cortical and trabecular regions of interest were evaluated using Microview (v. 2.2, GE Healthcare, London, ON, Canada). The trabecular region of interest began 270 μm proximal to the distal growth plate and extended proximally for 10% of the total length of the bone (Bouxsein et al., 2010). For the trabecular bone region, we assessed bone volume fraction (BV/TV, %), trabecular thickness (Tb.Th, μm), trabecular separation (TbSp, μm), trabecular number (Tb.N, 1/mm), and connectivity density (Conn.D 1/mm^3). The cortical region of interest consisted of 50 slices centered at the femoral midshaft. Cortical bone parameters included the total cross-sectional area, cortical bone area (TA and BA, mm^2), bone area fraction (BA/TA, %), cortical thickness (mm), maximum and minimum area moments of inertia (I_{max} and I_{min}, mm^4), and polar moment of inertia (J). All methods followed American Society for Bone and Mineral Research guidelines (Bouxsein et al., 2010).

2.9 | Bone strength testing

After completion of μCT, the strength of the femoral midshaft was assessed by four-point bending using previously described methods (Sinder et al., 2015; Smith, Bigelow, & Jepsen, 2013). Briefly, frozen specimens were thawed in calcium-buffered saline. A low-force mechanical testing system (858 Minibionix II; MTS Systems Corporation, Eden Prairie, MN, USA) was used to apply a constant displacement rate of 0.05 mm/s in the anterior–posterior direction, with the anterior side in compression. Upper and lower supports were 2.075 and 6.35 mm apart, respectively. Force–displacement data were used to determine structural properties (maximum load, stiffness, and postyield displacement). Mechanical stiffness from four-point bending was adjusted for μCT-derived femoral midshaft area moment of inertia to calculate estimated material properties (Jepsen, Silva, Vashishth, Guo, & van der Meulen, 2015).

2.10 | Statistical analysis

Statistical analyses were run in SPSS 24 (IBM, Armonk, NY) using general linear models to test for effects of temperature and/or a temperature × age interaction. If there was a significant effect of temperature or temperature × age for a particular variable, the GLM was stratified by age to obtain p values for temperature (20 °C vs 22 °C vs 26 °C) within mice at 6 or 12 weeks of age. Given the influence of body mass on long bone cortical cross-sectional geometry, femoral cortical variables (Ct.Th, Ct.Ba, Ct.TA, I_{max}, I_{min}, J) were adjusted by regressing against body mass and testing for significance using the residuals (Lang et al., 2005). The significance level for major effects was set at alpha = 0.05. All graphs were made using GraphPad Prism 7.0c for Mac OSX (GraphPad Software, La Jolla, CA).

3 | RESULTS

3.1 | Body size and composition, whole-body BMD, and hormone levels

Body mass and femur length did not differ across housing temperatures (Figure 1a and Table 1), although at 6, 9, and 12 weeks of age, cool mice ate 12%, 36%, and 27% more than control mice and 22%, 70%, and 53% more than warm mice, respectively (p < .005 for all, Figure 1b). Cool mice had shorter bodies at 9 and 12 weeks of age (p < .05 for both, Figure 1c) and shorter tails at 6, 9, and 12 weeks of age (p < .05 for all, Table 1).

Longitudinal DXA showed differences in body composition across temperatures. BMD was 5.1% lower in cool versus control mice at 6 weeks of age (p < .01) but not 9 or 12 weeks of age (Figure 1d). BMC (g) did not differ at any age (Table 1). Compared to control and warm mice, cool mice had lower %body fat at 6 weeks of age but not at 9 or 12 weeks of age (Figure 1e), while lean mass did not differ between groups (Table 1). Serum leptin was lower in cool and control versus warm mice at 6 weeks and in cool versus warm mice at 12 weeks of age (p < .05 for all, Figure 1f).

3.2 | Trabecular bone at distal femur and cortical bone at midshaft femur

In the distal femur, there were no effects of temperature on trabecular bone microarchitecture at 6 weeks of age. At 12 weeks of age, trabecular bone volume fraction was 29%–31% lower (p < .05, Figure 2a,b) and connectivity density was 14%–23% lower in control and cool versus warm housed mice, respectively (p < .05 for both, Figure 2c). Cool mice also had 9% lower trabecular number and 9% higher trabecular

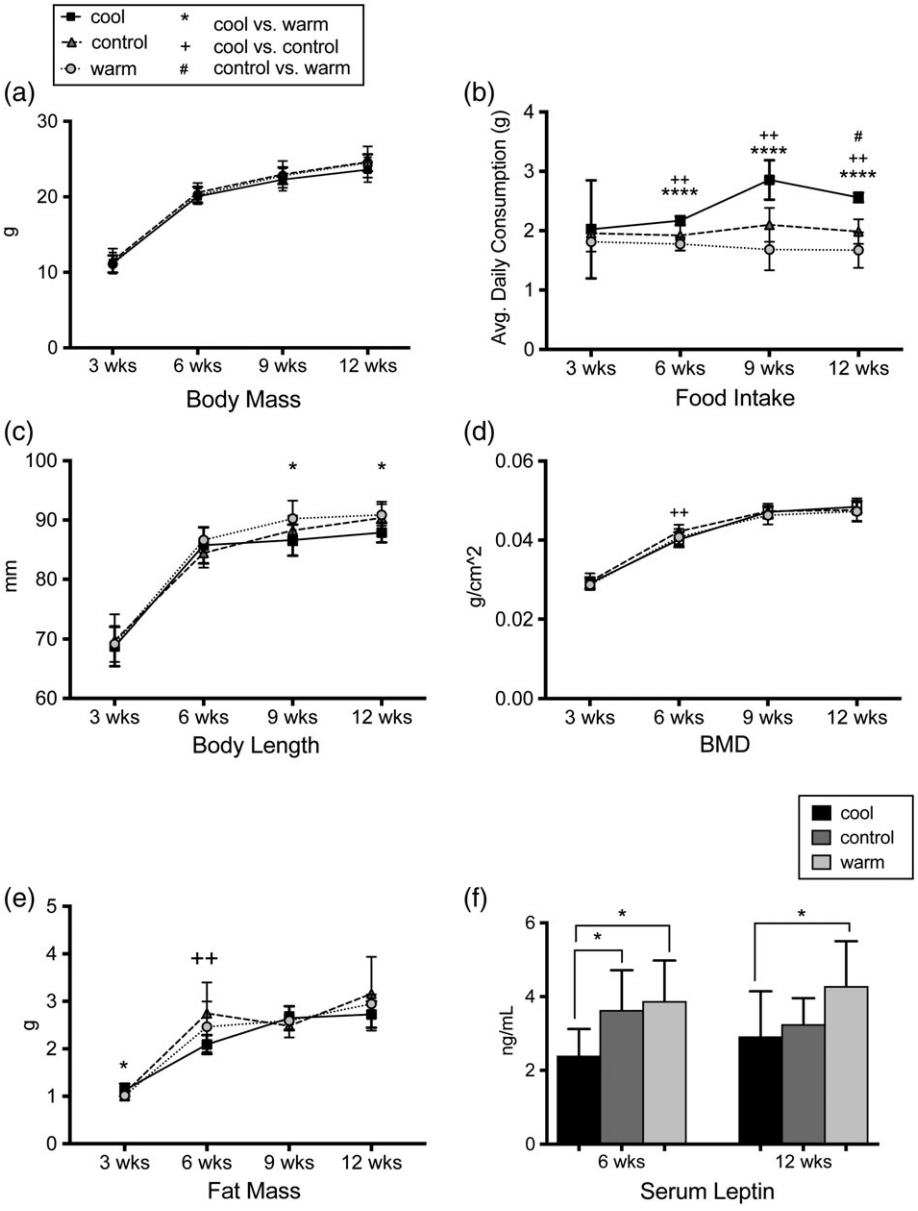

FIGURE 1 (a) Body mass did not differ by temperature (N = 8/group). (b) Cool versus warm mice ate more at 6, 9, and 12 weeks (p < .0001 for all, N = 4 cages/group). (c) Cool versus warm mice had shorter bodies at 9 and 12 weeks (p < .05, N = 8/group). (d) Bone mineral density was lower in cool versus control mice at 6 weeks (p = .009) but did not otherwise differ (N = 8/group). (e) Cool versus control mice had lower fat mass at 6 weeks (p = .002, N = 8/group). (f) Cool versus warm mice had lower serum leptin at 6 and 12 weeks and control versus warm mice had lower serum leptin at 6 weeks (p < .05, N = 8/group). Error bars represent ±1*SD*

spacing (p < .05 for both, Table 2) versus warm mice, but there were no significant effects of temperature on trabecular thickness (Table 2).

In midshaft femur cortical bone cross-sectional geometry, there were no significant differences across temperatures at 6 weeks of age. At 12 weeks of age, cortical bone area fraction was 6% lower in cool mice (p < .05, Figure 2a,d), and cortical bone thickness was lower in control (p < .05) but not cool (p = .053) versus warm mice (Figure 2e). Other cortical bone properties, including cortical bone area, total area, I_{max}, I_{min}, and J, did not differ across temperatures (Table 2).

3.3 | Bone marrow adiposity and bone strength

Histology of the distal femur showed that the number (Ad.N/BS) and volume (Ad.V/TV) of adipocytes in the marrow cavity were highly variable across individuals and were not affected by temperature (Table 3). Mechanical testing of the femoral diaphysis indicated no temperature-induced differences in stiffness, maximum load, or post-yield displacement (Table 3).

3.4 | UCP1 mRNA and protein in brown adipose tissue

As measured by RT-PCR, the relative mRNA abundance of the nonshivering thermogenesis marker UCP1 in BAT was 58% higher for cool versus warm mice at 6 weeks of age (p < .05) and 66%–68% higher in cool and control versus warm mice 12 weeks of age p < .005 for both, N = 8 individuals/group, Figure 3). Following RT-PCR, a subset of mice was used for UCP1 protein detection via Western blotting (N = 3–4

TABLE 1 Body length, bone mineral content, and body composition in male C57BL/6J mice housed at 20, 22, or 26 °C from 3 weeks to 6 or 12 weeks of age (N = 8/group)

	6 weeks of age						9 weeks of age						12 weeks of age						p_{temp} 6 weeks	p_{temp} 9 weeks	p_{temp} 12 weeks
	20 °C (cool)		22 °C (control)		26 °C (warm)		20 °C (cool)		22 °C (control)		26 °C (warm)		20 °C (cool)		22 °C (control)		26 °C (warm)				
	Mean	*SD*	Mean	*SD*	Mean	*SD*	Mean	*SD*	Mean	*SD*	Mean	*SD*	Mean	*SD*	Mean	*SD*	Mean	*SD*			
Femur length (mm)	14.2	0.10	14.2	0.40	14.0	0.40	N/A		N/A		N/A		15.5	0.8	15.6	0.2	15.6	0.1	NS	NS	NS
Tail length (mm)	69.9*	3.4	73.4*	2.8	75.8	2.3	75.8*	2.1	76.4	1.6	78.5	2.6	75.0*	2.9	78.0	4.2	81.6	2.9	<.0001	.041	.004
BMC (g)	0.309	0.022	0.310	0.023	0.310	0.016	0.384	0.034	0.392	0.022	0.388	0.018	0.413	0.036	0.441	0.065	0.421	0.014	NS	NS	NS
Lean mass (g)	15.99	0.99	16.58	1.31	16.13	1.22	17.52	1.41	18.24	1.43	17.79	1.05	18.58	1.38	19.15	1.33	19.21	0.95	NS	NS	NS

from each temperature, Figure 3). UCP1 protein expression in BAT total protein lysate was 50%–55% higher in cool and control versus warm mice at 6 weeks and 66% higher in cool versus warm mice at 12 weeks of age (p < .01 for all, Figure 3).

4 | DISCUSSION

In this study, we tested two hypotheses: (1) that exposure to low temperature impairs bone acquisition during rapid skeletal growth and (2) that upregulation of UCP1 is proportional to the decrease in temperature. We predicted that low temperature would increase sympathetic tone, leading to decreased trabecular microarchitecture, cortical bone cross-sectional geometry, and bone strength, but also higher UCP1 expression as a marker of NST in BAT. To test these hypotheses, we raised 3-week-old C57BL/6J male mice to 6 or 12 weeks of age at 20 °C (low temperature, "cool"), 22 °C (standard housing, "control"), and 26 °C (near thermoneutrality, "warm").

In partial support of our first hypothesis, the results indicate that low temperature was deleterious to overall skeletal size and to bone mass. Compared to mice housed near thermoneutrality, cool-housed mice had shorter bodies and tails, lower trabecular bone volume fraction, sparser, less connected trabeculae in the distal femur, lower midshaft femur cortical bone volume fraction, and a trend toward lower cortical thickness (p = .053), at 12 weeks of age. Despite higher food intake, cool mice had lower fat mass at 6 weeks of age and lower serum leptin levels at 6 and 12 weeks, although their body mass did not differ from warm-housed mice.

Contrary to our first hypothesis, cool-housed mice did not have lower BMD, higher marrow adiposity, or lower midshaft diaphyseal bone strength. The most likely explanation is that the range of temperatures we used was too small. In terms of bone strength, cool housed mice had thinner cortices but not lower polar moments of inertia, indicating that the distribution of bone mass allowed maintenance of bending strength. More generally, the finding that a modest temperature change had greater effects in trabecular than cortical bone is consistent with the observation that trabecular bone is more responsive than cortical bone to external stimuli, perhaps due to its relatively higher surface area and turnover rate (Bilezikian, Raisz, & Rodan, 2002). Similarly, although Huggins and Blocksom (1936) found that transplanting vertebrae from the tail to the abdominal cavity of rats decreased marrow adiposity, the temperature difference from outside to inside the body was greater than the range of temperatures used here.

In support of our second hypothesis, low temperature upregulated nonshivering thermogenesis. At 6 weeks of age, cool mice had significantly more UCP1 mRNA and cool and control mice had significantly more UCP1 protein compared to warm mice. At 12 weeks of age, cool and control mice had significantly more UCP1 mRNA, and cool mice had significantly more UCP1 protein compared to warm mice. The mRNA values reflect transcription of the gene, while protein levels reflect its existing expression. This pattern shows that mice at both 20 and 22 °C had chronically increased UCP1 activity in response to these temperatures. Although this relatively modest 6 °C difference between cool and warm housing temperatures was

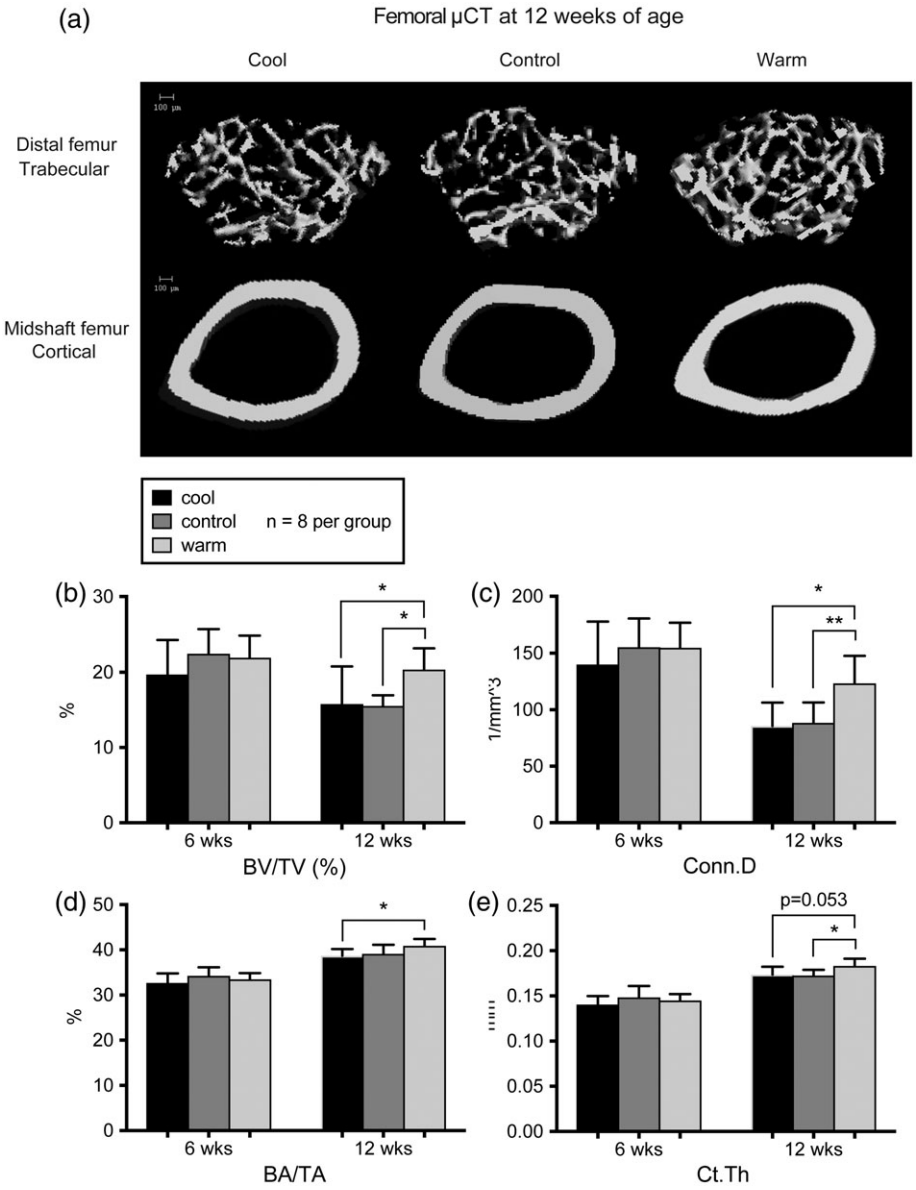

FIGURE 2 (a) MicroCT reconstructions of trabecular bone in the distal femur and cortical bone in the midshaft femur. (b) In the distal femur, trabecular bone volume fraction (BV/TV) was lower for cool and control versus warm mice at 12 weeks ($p < .05$). (c) Connectivity density was lower for cool and control mice versus warm at 12 weeks ($p = .03$ and $p = .008$). (d) In the cortical midshaft femur, bone area fraction (BA/TA) of cool mice was lower than warm mice ($p = .041$) at 12 weeks. (e) Cortical thickness at 12 weeks was significantly lower in control versus warm ($p = .03$) but not cool versus warm mice ($p = .053$). There were no significant differences at 6 weeks of age. Error bars represent 1 *SD*. *N* = 8/group for all data shown

sufficient to increase UCP1 expression but insufficient to restore normal bone architecture, it is possible that bone loss would have been even greater in its absence. Alternatively, it is possible that UCP1 upregulation helps to maintain temperature homeostasis, but that being warmer does not help to preserve bone mass.

4.1 | Comparison to previous studies of temperature and bone in animal models

These data are consistent with older studies demonstrating reduced longitudinal growth, bone length, and tail length in experimental animals housed at sub-thermoneutral temperatures (Al-Hilli & Wright, 1983; Ashoub, 1958; Sumner, 1909; Weaver & Ingram, 1969). More recently, Serrat, King, and Lovejoy (2008) and Serrat (2013) found that mice housed at 7 °C had shorter bodies, tails, and limb bones than mice raised at 27 °C, despite higher food intake and no difference in body mass. Importantly, cold exposure reduced blood flow and solute transport to limb bone growth plates in vivo (Serrat et al., 2008; Serrat, Williams, & Farnum, 2009), whereas cold-induced reductions in growth were mitigated by exercise (Serrat, Williams, & Farnum, 2010) and hindlimb heating (Serrat, 2014; Serrat et al., 2015). These studies strongly suggest circulation to the growth plate underlies temperature-induced differences in limb length, and reduced circulation may contribute to the decreased trabecular bone architecture we

TABLE 2 Distal femoral trabecular bone microarchitecture and midshaft femoral cortical bone cross-sectional geometry in male C57BL/6J mice housed at 20, 22, or 26 °C from 3 weeks to 6 or 12 weeks of age (*N* = 8/group)

	6 weeks of age						12 weeks of age						
	20 °C (cool)		22 °C (control)		26 °C (warm)		20 °C (cool)		22 °C (control)		26 °C (warm)		
	Mean	*SD*	Mean	*SD*	Mean	*SD*	Mean	*SD*	Mean	*SD*	Mean	*SD*	$p_{temperature}$
Distal femur trabecular bone													
BV/TV (%)	19.7	4.6	22.5	3.3	22.0	2.9	15.8*	5.0	15.5*	1.4	20.4	2.8	.031
Tb.N (/mm)	5.57	0.62	5.68	0.24	5.83	0.34	4.92*	0.30	5.03	0.24	5.35	0.34	.035
Tb.Th (mm)	0.058	0.004	0.063	0.007	0.061	0.005	0.057	0.008	0.056	0.002	0.062	0.005	NS
Tb.Sp (mm)	0.179	0.022	0.174	0.010	0.169	0.010	0.198*	0.015	0.195	0.011	0.180	0.011	.018
Conn.D (/mm)	0.327	0.021	0.343	0.019	0.335	0.014	0.387*	0.015	0.391*	0.020	0.409	0.015	.019
Midshaft femur cortical bone													
BA/TA (%)	32.7	2.1	34.3	1.9	33.5	1.4	38.7*	1.5	39.1	2.0	40.9	1.5	.037
BA (mm^2)	0.59	0.04	0.63	0.06	0.62	0.04	0.74	0.07	0.73	0.03	0.78	0.03	NS
TA (mm^2)	1.80	0.05	1.84	0.10	1.84	0.10	1.92	0.17	1.88	0.10	1.91	0.07	NS
Ct.Th (mm)	0.140	0.009	0.148	0.013	0.145	0.007	0.174#	0.009	0.173*	0.006	0.183	0.008	.022
Imax (mm^4)	0.177	0.016	0.197	0.032	0.191	0.026	0.238	0.044	0.236	0.030	0.260	0.017	NS
Imin (mm^4)	0.093	0.005	0.098	0.014	0.097	0.009	0.118	0.023	0.110	0.009	0.115	0.011	NS
J (mm^4)	0.269	0.021	0.295	0.044	0.289	0.034	0.356	0.066	0.346	0.036	0.374	0.026	NS

*Significant difference versus warm ($p < .05$, GLM and Tukey test). #$p = .053$

observed. In this study, mice housed at 20–22 °C had shorter bodies and tails but not shorter femurs than mice at 26 °C. As noted above, the low temperature we used was sufficient to change growth of the most distal extremities (e.g., the tail), but may not have been enough to affect limb bone growth. The shorter overall body length could reflect a combination of decreased skull and/or vertebral length, which we will measure in future studies. It should also be noted that although femur length did not change, trabecular bone volume in the distal femur was significantly lower, demonstrating that temperature can affect internal bone architecture without altering the external appearance of the bone. Consistent with our findings, Iwaniec et al. (2016) showed that housing mice at thermoneutrality (32 °C) rather than the standard housing temperature of 22 °C slowed the rate of age-related trabecular bone loss, demonstrating that even a mild temperature decrease is deleterious to the skeleton.

There is growing evidence that the mechanism underlying such cold-induced bone loss involves upregulation of sympathetic tone. Cold exposure increases sympathetic nervous system (SNS) activation in mammals, leading to warming mechanisms such as shivering, piloerection, vasoconstriction, and nonshivering thermogenesis in BAT. However, multiple studies in animal models have shown that chronic SNS activation also induces bone loss via β-adrenergic receptors expressed on osteoblasts, such that mice lacking the beta2-adrenergic receptor are protected from bone loss (Bonnet, Pierroz, & Ferrari, 2008; Kajimura et al., 2011). Most compellingly, the *Misty* mouse strain has dysfunctional BAT, high sympathetic tone, and low bone mass, the latter of which is reduced when mice are treated with the beta-adrenergic antagonist propranolol (Motyl et al., 2013). These data suggest that nonshivering thermogenesis in BAT might protect the skeleton by warming the organism and therefore reducing SNS-induced bone loss (Motyl & Rosen, 2011).

Fewer studies have addressed the effects of sympathetic tone on bone mass in humans, although it has been noted that patients taking "beta blocker" drugs, which inhibit sympathetic signaling to osteoblast beta2-adrenergic receptors, have higher BMD and lower risk of fracture compared to the background population (Bonnet et al., 2007; Yang, Nguyen, Eisman, & Nguyen, 2012). More generally, multiple studies have shown that BAT is associated with higher bone mass in humans, including higher femoral total area and bone cross-sectional area in both men and women of varying BMI and age, and BMD in

TABLE 3 Distal femoral marrow adiposity at 12 weeks of age (*N* = 4-5/group) and midshaft femoral bone strength testing at 6 and 12 weeks of age (*N* = 8/group) in male C57BL/6J mice housed at 20, 22, or 26 °C beginning at 3 weeks of age

	6 weeks of age						12 weeks of age						
	20 °C (cool)		22 °C (control)		26 °C (warm)		20 °C (cool)		22 °C (control)		26 °C (warm)		
	Mean	*SD*	Mean	*SD*	Mean	*SD*	Mean	*SD*	Mean	*SD*	Mean	*SD*	$p_{temperature}$
Ad.N/BS (%)	59.4	43.0	32.6	16.2	44.1	26.2	N/A		N/A		N/A		NS
Ad.V/TV (%)	0.34	0.19	0.22	0.16	0.24	0.16	N/A		N/A		N/A		NS
Maximum load (N)	17.6	1.6	19.0	1.5	19.2	1.3	22.9	3.5	24.2	4.2	24.0	2.7	NS
Stiffness (N/mm)	101.6	12.1	115.0	13.8	109.6	9.5	170.8	30.3	176.6	29.2	178.3	17.0	NS
Postyield displacement (mm)	0.70	0.35	0.93	0.31	0.80	0.29	0.44	0.21	0.62	0.44	0.54	0.35	NS
Estimated elastic modulus (GPa)	4.23	0.49	4.56	0.56	4.37	0.49	5.62	0.74	6.26	1.31	6.06	0.85	NS

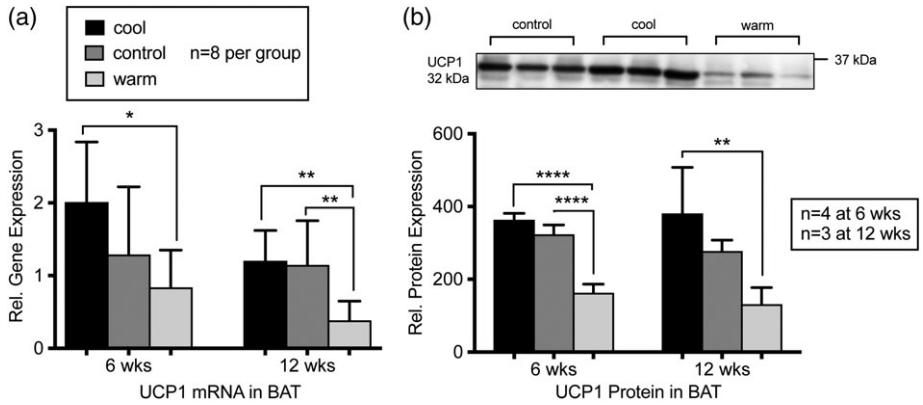

FIGURE 3 (a) Relative mRNA of NST marker UCP1 in BAT by qRT-PCR was significantly higher for cool versus warm mice at 6 (p = .017) and 12 weeks (p = .004). UCP1 mRNA was also increased in control versus warm mice at 12 weeks (p = .005) with N = 8 individuals per group. (b) Western blot of UCP1 from BAT total protein lysate shows increased expression for cool versus warm mice at 6 (n = 4 per group, p < .001) and 12 weeks (N = 3 per group, p = .009) and for control versus warm mice at 6 weeks (N = 4 per group, p < .001). Representative blot with anti-UCP1 signal shown for 12 weeks BAT with one individual per lane. Error bars represent 1 *SD*

lean, young women (Bredella et al., 2012, 2014; Lee et al., 2013). BAT mass is highest in humans during adolescent peak bone mass acquisition, and as in adults, is positively correlated with femoral cortical bone area and total cross-sectional area in children and adolescents (Gilsanz et al., 2012; Ponrartana et al., 2012). However, more work is needed to understand how interactions between BAT and the skeleton affect bone mass, and to test the role of other factors such as muscle mass.

4.2 | Relevance for understanding how temperature affects bone in humans

In humans, high-latitude populations under chronic cold exposure generally exhibit a wider pelvis, shorter stature, and shorter distal limb segments, as well as lower bone density and cortical thickness and accelerated rates of bone loss, compared to lower latitude populations (Harper et al., 1984; Katzmarzyk & Leonard, 1998; Lazenby, 1997; Leslie et al., 2006; Leslie et al., 2008; Mazess & Mather, 1974; Mazess & Mather, 1975; Pearson, 2000; Roberts, 1953; Ruff, 1994; Thompson & Gunness-Hey, 1981; Wallace et al., 2014). For example, skeletal analyses and bone mineral density values suggested earlier onset of age-related bone loss in indigenous cold-dwelling populations versus populations of European ancestry (Harper et al., 1984; Mazess & Mather, 1974, 1975; Thompson & Gunness-Hey, 1981; Wallace et al., 2014). However, the extent of bone loss attributable to cold exposure is difficult to disentangle from other factors, including ancestry, consumption of a high-protein, low-calcium diet (Mazess & Mather, 1974), and metabolic changes such as cold-induced hyperthyroidism (Lazenby, 1997). Hyperthyroidism is particularly interesting in this context because elevated thyroid hormone is a stimulus of NST in BAT, and previous studies have shown that hyperthyroidism in response to chronic cold exposure, known as the polar T3 syndrome, both increases sympathetic tone and accelerates bone turnover (Allain & McGregor, 1993; Schneider, Barrett-Connor, & Morton, 1994, 1995). It is also interesting to note that accelerated bone loss in cold-dwelling humans appears as early as the fourth decade of life, at around the same age when studies of cold-responsive BAT suggest its abundance begins to decline (Harper et al., 1984; Mazess & Mather, 1974, 1975; Wallace et al., 2014).

Although more work is needed to determine the timing and extent of bone loss with age in cold-dwelling humans, the reported patterns are generally consistent with our findings in the mouse model. In cool housed mice, the decrements in bone volume fraction, trabecular number, and connectivity density versus warm housed mice are greater in 12-week-old versus 6-week-old animals, similar to the accelerated age-related bone loss seen in humans. However, in young, rapidly growing mice up to 12 weeks of age, low temperature is more deleterious to trabecular bone microarchitecture than it is to bone mineral density or cortical bone properties, whereas in aging humans, cold decreases cortical bone thickness and BMD. Studies of old cool-exposed mice are needed to determine how low temperature affects the aging skeleton. More generally, impaired bone acquisition occurred in spite of higher uncoupling protein expression in brown adipose tissue, suggesting that although higher brown adipose tissue mass is linked to higher bone mass both in humans and in animal models, it is insufficient to normalize bone acquisition during chronic exposure to low temperature. Our results also demonstrate that developmental plasticity of the skeleton during subadult growth can occur in response to temperature as well as to mechanical loading, and thus climate may underlie some of the phenotypic variation observed among human populations.

4.3 | Limitations and future directions

There are several limitations to this study. First, we assessed only males and used a single mouse strain, and it is possible that there are strain-specific and/or sex-specific responses to temperature. Second, as discussed above, the narrow range of temperature variation we used likely diminished the differences among our experimental groups. In addition, it is not clear whether the relationship between temperature and bone is linear or whether there are thresholds for the entire body or for particular regions. These questions will be addressed in future work focused on comparisons between temperature and bone growth in specific skeletal regions. Third, we raised mice only to

12 weeks of age, and therefore were not able to assess how low temperature and UCP1 upregulation affect the skeleton during aging. Finally, we did not directly measure sympathetic tone or body temperature in the mice. Future studies will use mouse enclosures that generate greater temperature differences and will include quantification of additional outcomes such as body temperature, activity level, energy expenditure, and metabolism.

5 | CONCLUSION

In this study, we sought to test the developmental plasticity of cortical and trabecular bone in response to low temperature. We hypothesized that low temperature would induce proportional decreases in cortical and trabecular bone acquisition, as well as proportional increases in nonshivering thermogenesis in BAT. In support of our hypotheses, cool-housed mice had lower trabecular bone mass in the femur compared to warm housed mice, despite greater food intake and increased UCP1 expression in BAT. These results support the hypothesis that the growing skeleton has phenotypic plasticity in response to temperature. Upregulation of UCP1 in brown adipose tissue leading to increased nonshivering thermogenesis may have mitigated bone loss but was not sufficient to prevent it.

ACKNOWLEDGMENTS

AR and MD planned experiments and drafted the article. AR, CT, MD, MC, CM, LS, TS, and TB performed experiments, collected data, and analyzed data. MC, CM, LS, TS, and TB reviewed and edited the article. Funding for this project was provided by NSF BCS-1638553 to MD. Research reported in this publication was supported by the National Institute of Arthritis and Musculoskeletal and Skin Diseases of the National Institutes of Health under Award Number P30 AR069620. The content is solely the responsibility of the authors and does not necessarily represent the official views of the National Institutes of Health. The authors thank Paul Thurmond, Elizabeth Vernasco-Price, Joseph Sanders, and Kathie Hutyra for assistance with mouse experiments. They are grateful to Drs Alon Kahana, Phillip E. Kish, and Alfonso Saera-Vila for assistance with protein and mRNA experiments. They thank two anonymous reviewers for helpful comments that improved the article.

ORCID

Maureen J. Devlin http://orcid.org/0000-0003-0845-3090

REFERENCES

Aguirre, J. I., Leal, M. E., Rivera, M. F., Vanegas, S. M., Jorgensen, M., & Wronski, T. J. (2007). Effects of basic fibroblast growth factor and a prostaglandin E2 receptor subtype 4 agonist on osteoblastogenesis and adipogenesis in aged ovariectomized rats. *Journal of Bone and Mineral Research: The Official Journal of the American Society for Bone and Mineral Research*, *22*(6), 877–888.

Al-Hilli, F., & Wright, E. A. (1983). The effects of changes in the environmental temperature on the growth of bone in the mouse. Radiological and morphological study. *British Journal of Experimental Pathology*, *64*(1), 43–52.

Aldridge, G. M., Podrebarac, D. M., Greenough, W. T., & Weiler, I. J. (2008). The use of total protein stains as loading controls: An alternative to high-abundance single-protein controls in semi-quantitative immunoblotting. *Journal of Neuroscience Methods*, *172*(2), 250–254.

Allain, T. J., & McGregor, A. M. (1993). Thyroid hormones and bone. *The Journal of endocrinology*, *139*(1), 9–18.

Allen, J. A. (1877). The influence of physical conditions in the genesis of species. *Radical Review*, *1*, 108–140.

Ashoub, M. A. (1958). Effect of two extreme temperatures on growth and tail-length of mice. *Nature*, *181*(4604), 284.

Au-Yong, I. T., Thorn, N., Ganatra, R., Perkins, A. C., & Symonds, M. E. (2009). Brown adipose tissue and seasonal variation in humans. *Diabetes*, *58*(11), 2583–2587.

Bergmann, C. (1847). Ueber die verhaltnisse der warmeokonomie der thiere zu ihrer grosse. *Gottinger Studien*, *3*, 595–708.

Bilezikian, J. P., Raisz, L. G., & Rodan, G. A. (2002). *Principles of bone biology*. San Diego: Academic Press.

Bonnet, N., Gadois, C., McCloskey, E., Lemineur, G., Lespessailles, E., Courteix, D., & Benhamou, C. L. (2007). Protective effect of beta blockers in postmenopausal women: Influence on fractures, bone density, micro and macroarchitecture. *Bone*, *40*(5), 1209–1216.

Bonnet, N., Pierroz, D. D., & Ferrari, S. L. (2008). Adrenergic control of bone remodeling and its implications for the treatment of osteoporosis. *Journal of Musculoskeletal & Neuronal Interactions*, *8*(2), 94–104.

Bouxsein, M. L., Boyd, S. K., Christiansen, B. A., Guldberg, R. E., Jepsen, K. J., & Müller, R. (2010). Guidelines for assessment of bone microstructure in rodents using micro–computed tomography. *Journal of Bone and Mineral Research*, *25*(7), 1468–1486.

Bouxsein, M. L., Devlin, M. J., Glatt, V., Dhillon, H., Pierroz, D. D., & Ferrari, S. L. (2009). Mice lacking Beta-adrenergic receptors have increased bone mass, but are not protected from deleterious skeletal effects of ovariectomy. *Endocrinology*, *150*(1), 144–52.

Bouxsein, M. L., Pierroz, D. D., Glatt, V., Goddard, D. S., Cavat, F., Rizzoli, R., & Ferrari, S. L. (2005). Beta-Arrestin2 regulates the differential response of cortical and trabecular bone to intermittent PTH in female mice. *Journal of Bone and Mineral Research: The Official Journal of the American Society for Bone and Mineral Research*, *20*(4), 635–643.

Bredella, M. A., Fazeli, P. K., Freedman, L. M., Calder, G., Lee, H., Rosen, C. J., & Klibanski, A. (2012). Young women with cold-activated brown adipose tissue have higher bone mineral density and lower Pref-1 than women without brown adipose tissue: A study in women with anorexia nervosa, women recovered from anorexia nervosa, and normal-weight women. *The Journal of Clinical Endocrinology and Metabolism*, *97*(4), E584–E590.

Bredella, M. A., Gill, C. M., Rosen, C. J., Klibanski, A., & Torriani, M. (2014). Positive effects of brown adipose tissue on femoral bone structure. *Bone*, *58*, 55–58.

Cannon, B., & Nedergaard, J. (2011). Nonshivering thermogenesis and its adequate measurement in metabolic studies. *The Journal of Experimental Biology*, *214*(Pt 2), 242–253.

Churchill, S. E. (1998). Cold adaptation, heterochrony, and Neandertals. *Evolutionary Anthropology*, *7*(2), 46–61.

Cypess, A. M., Lehman, S., Williams, G., Tal, I., Rodman, D., Goldfine, A. B., et al. (2009). Identification and importance of brown adipose tissue in adult humans. *The New England Journal of Medicine*, *360*(15), 1509–1517.

David, J. M., Chatziioannou, A. F., Taschereau, R., Wang, H., & Stout, D. B. (2013). The hidden cost of housing practices: Using noninvasive imaging to quantify the metabolic demands of chronic cold stress of laboratory mice. *Comparative Medicine*, *63*(5), 386–391.

Dempster, D. W., Compston, J. E., Drezner, M. K., Glorieux, F. H., Kanis, J. A., Malluche, H., … Parfitt, A. M. (2013). Standardized nomenclature, symbols, and units for bone histomorphometry: A 2012 update of the report of the ASBMR Histomorphometry Nomenclature Committee. *Journal of Bone and Mineral Research: The Official Journal of the American Society for Bone and Mineral Research*, *28*(1), 2–17.

Devlin, M. J. (2015). The "skinny" on brown fat, obesity, and bone. *American Journal of Physical Anthropology*, *156*(Suppl 59), 98–115.

Devlin, M. J., Brooks, D. J., Conlon, C., Vliet, M., Louis, L., Rosen, C. J., & Bouxsein, M. L. (2016). Daily leptin blunts marrow fat but does not

impact bone mass in calorie-restricted mice. *The Journal of Endocrinology*, *229*(3), 295–306.

Devlin, M. J., Van Vliet, M., Motyl, K., Karim, L., Brooks, D. J., Louis, L., … Bouxsein, M. L. (2014). Early-onset type 2 diabetes impairs skeletal acquisition in the Male TALLYHO/JngJ mouse. *Endocrinology*, *155*(10), 3806–3,816.

Erikson, H., Krog, J., Andersen, K. L., & Scholander, P. F. (1956). The critical temperature in naked man. *Acta Physiologica Scandinavica*, *37*(1), 35–39.

Fischer, A. W., Cannon, B., & Nedergaard, J. (2018). Optimal housing temperatures for mice to mimic the thermal environment of humans: An experimental study. *Molecular Metabolism*, *7*, 161–170.

Foster, F., & Collard, M. (2013). A reassessment of Bergmann's rule in modern humans. *PLoS One*, *8*(8), e72269.

Gaskill, B. N., Gordon, C. J., Pajor, E. A., Lucas, J. R., Davis, J. K., & Garner, J. P. (2012). Heat or insulation: Behavioral titration of mouse preference for warmth or access to a nest. *PLoS One*, *7*(3), e32799.

Gilda, J. E., & Gomes, A. V. (2013). Stain-free total protein staining is a superior loading control to beta-actin for western blots. *Analytical Biochemistry*, *440*(2), 186–188.

Gilsanz, V., Smith, M. L., Goodarzian, F., Kim, M., Wren, T. A., & Hu, H. H. (2012). Changes in brown adipose tissue in boys and girls during childhood and puberty. *The Journal of Pediatrics*, *160*(4), 604–609 e601.

Gordon, C. J. (2012). Thermal physiology of laboratory mice: Defining thermoneutrality. *Journal of Thermal Biology*, *37*(8), 654–685.

Hardy, J. D., & Dubois, E. F. (1937). Regulation of heat loss from the human body. *Proceedings of the National Academy of Sciences of the United States of America*, *23*(12), 624–631.

Harper, A. B., Laughlin, W. S., & Mazess, R. B. (1984). Bone mineral content in St. Lawrence Island Eskimos. *Human Biology*, *56*(1), 63–78.

Heaton, J. M. (1972). The distribution of brown adipose tissue in the human. *Journal of Anatomy*, *112*(Pt 1), 35–39.

Hildebrand, T., Laib, A., Muller, R., Dequeker, J., & Ruegsegger, P. (1999). Direct three-dimensional morphometric analysis of human cancellous bone: Microstructural data from spine, femur, iliac crest, and calcaneus. *Journal of Bone and Mineral Research: The Official Journal of the American Society for Bone and Mineral Research*, *14*(7), 1167–1174.

Hildebrand, T., & Rüegsegger, P. (1997). A new method for the model independent assessment of thickness in three-dimensional images. *Journal of Microscopy*, *185*, 67–75.

Holliday, T. W. (1997). Body proportions in late Pleistocene Europe and modern human origins. *Journal of Human Evolution*, *32*(5), 423–448.

Holliday, T. W., & Hilton, C. E. (2010). Body proportions of circumpolar peoples as evidenced from skeletal data: Ipiutak and Tigara (point hope) versus Kodiak Island Inuit. *American Journal of Physical Anthropology.*, *142*(2), 287–302.

Huggins, C., & Blocksom, B. H. (1936). Changes in outlying bone marrow accompanying a local increase of temperature within physiological limits. *Journal of Experimental Medicine*, *64*(2), 253–274.

Huttunen, P., Hirvonen, J., & Kinnula, V. (1981). The occurrence of brown adipose tissue in outdoor workers. *European Journal of Applied Physiology and Occupational Physiology*, *46*(4), 339–345.

Iwaniec, U. T., Philbrick, K. A., Wong, C. P., Gordon, J. L., Kahler-Quesada, A. M., Olson, D. A., et al. (2016). Room temperature housing results in premature cancellous bone loss in growing female mice: Implications for the mouse as a preclinical model for age-related bone loss. *Osteoporosis International*, *27*(10), 3091–3,101.

Jepsen, K. J., Silva, M. J., Vashishth, D., Guo, X. E., & van der Meulen, M. C. (2015). Establishing biomechanical mechanisms in mouse models: Practical guidelines for systematically evaluating phenotypic changes in the diaphyses of long bones. *Journal of Bone and Mineral Research: The Official Journal of the American Society for Bone and Mineral Research*, *30*(6), 951–966.

Kajimura, D., Hinoi, E., Ferron, M., Kode, A., Riley, K. J., Zhou, B., … Karsenty, G. (2011). Genetic determination of the cellular basis of the sympathetic regulation of bone mass accrual. *Journal of Experimental Medicine*, *208*(4), 841–851.

Karp, C. L. (2012). Unstressing intemperate models: How cold stress undermines mouse modeling. *Journal of Experimental Medicine*, *209*(6), 1069–1,074.

Katzmarzyk, P. T., & Leonard, W. R. (1998). Climatic influences on human body size and proportions: Ecological adaptations and secular trends. *American Journal of Physical Anthropology*, *106*(4), 483–503.

Kingma, B., Frijns, A., & van Marken Lichtenbelt, W. (2012). The thermoneutral zone: Implications for metabolic studies. *Frontiers in Bioscience*, *4*, 1975–1985.

Kingma, B. R., Frijns, A. J., Schellen, L., & van Marken Lichtenbelt, W. D. (2014). Beyond the classic thermoneutral zone: Including thermal comfort. *Temperature (Austin)*, *1*(2), 142–149.

Lang, D. H., Sharkey, N. A., Lionikas, A., Mack, H. A., Larsson, L., Vogler, G. P., et al. (2005). Adjusting data to body size: A comparison of methods as applied to quantitative trait loci analysis of musculoskeletal phenotypes. *Journal of Bone and Mineral Research: The Official Journal of the American Society for Bone and Mineral Research*, *20*(5), 748–757.

Lazenby, R. A. (1997). Bone loss, traditional diet, and cold adaptation in Arctic populations. *American Journal of Human Biology*, *9*(3), 329–341.

Lee, P., Brychta, R. J., Collins, M. T., Linderman, J., Smith, S., Herscovitch, P., … Celi, F. S. (2013). Cold-activated brown adipose tissue is an independent predictor of higher bone mineral density in women. *Osteoporosis International*, *24*(4), 1513–1518.

Leonard, W. R., & Levy, S. B. (2015). Contributions of brown adipose tissue to human metabolic adaptation: Comparative and evolutionary perspectives. *American Journal of Physical Anthropology*, *156*(S60):202.

Leslie, W. D., Metge, C. J., Weiler, H. A., Doupe, M., Wood Steiman, P., & O'Neil, J. D. (2006). Bone density and bone area in Canadian aboriginal women: The first nations bone health study. *Osteoporosis International*, *17*(12), 1755–1762.

Leslie, W. D., Weiler, H. A., Lix, L. M., & Nyomba, B. L. (2008). Body composition and bone density in Canadian white and aboriginal women: The first nations bone health study. *Bone*, *42*(5), 990–995.

Livak, K. J., & Schmittgen, T. D. (2001). Analysis of relative gene expression data using real-time quantitative PCR and the 2(−Delta Delta C [T]) method. *Methods*, *25*(4), 402–408.

Lodhi, I. J., & Semenkovich, C. F. (2009). Why we should put clothes on mice. *Cell Metabolism*, *9*(2), 111–112.

Lowell, B. B., & Spiegelman, B. M. (2000). Towards a molecular understanding of adaptive thermogenesis. *Nature*, *404*(6778), 652–660.

Mazess, R. B., & Mather, W. (1974). Bone mineral content of north Alaskan Eskimos. *The American Journal of Clinical Nutrition*, *27*(9), 916–925.

Mazess, R. B., & Mather, W. E. (1975). Bone mineral content in Canadian Eskimos. *Human Biology*, *47*(1), 44–63.

Meinel, L., Fajardo, R., Hofmann, S., Langer, R., Chen, J., Snyder, B., … Kaplan, D. (2005). Silk implants for the healing of critical size bone defects. *Bone*, *37*(5), 688–698.

Motyl, K. J., Bishop, K. A., DeMambro, V. E., Bornstein, S. A., Le, P., Kawai, M., et al. (2013). Altered thermogenesis and impaired bone remodeling in misty mice. *Journal of Bone and Mineral Research: The Official Journal of the American Society for Bone and Mineral Research*, *28*(9), 1885–1897.

Motyl, K. J., & Rosen, C. J. (2011). Temperatures rising: Brown fat and bone. *Discovery Medicine*, *11*(58), 179–185.

Murray, I., Havel, P. J., Sniderman, A. D., & Cianflone, K. (2000). Reduced body weight, adipose tissue, and leptin levels despite increased energy intake in female mice lacking acylation-stimulating protein. *Endocrinology*, *141*(3), 1041–1049.

Nagy, T. R., Krzywanski, D., Li, J., Meleth, S., & Desmond, R. (2002). Effect of group vs. single housing on phenotypic variance in C57BL/6J mice. *Obesity Research*, *10*(5), 412–415.

Nicholls, D. G., & Rial, E. (1999). A history of the first uncoupling protein, UCP1. *Journal of Bioenergetics and Biomembranes*, *31*(5), 399–406.

Overton, J. M. (2010). Phenotyping small animals as models for the human metabolic syndrome: Thermoneutrality matters. *International Journal of Obesity*, *34*(Suppl 2), S53–S58.

Pearson, O. M. (2000). Activity, climate, and postcranial robusticity: Implications for modern human origins and scenarios of adaptive change. *Current Anthropologyl*, *41*(4), 569–607.

Ponrartana, S., Aggabao, P. C., Hu, H. H., Aldrovandi, G. M., Wren, T. A., & Gilsanz, V. (2012). Brown adipose tissue and its relationship to bone structure in pediatric patients. *The Journal of Clinical Endocrinology and Metabolism*, *97*(8), 2693–2,698.

Ridler, T., & Calvard, S. (1978). Picture thresholding using an iterative selection method. *IEEE Transactions on Systems, Man, and Cybernetics*, *SMC-8*(8), 630–632.

Roberts, D. F. (1953). Body weight, race, and climate. *American Journal of Physical Anthropology*, *11*, 533–558.

Ruff, C. (2002). Variation in human body size and shape. *Annual Review of Anthropology*, *31*(1), 211–232.

Ruff, C. B. (1993). Climatic adaptation and hominid evolution: The thermoregulatory imperative. *Evolutionary Anthropology*, *2*, 53–60.

Ruff, C. B. (1994). Morphological adaptation to climate in modern and fossil hominids. *American Journal of Physical Anthropology*, *37*(S19), 65–107.

Saito, M., Okamatsu-Ogura, Y., Matsushita, M., Watanabe, K., Yoneshiro, T., Nio-Kobayashi, J., et al. (2009). High incidence of metabolically active brown adipose tissue in healthy adult humans: Effects of cold exposure and adiposity. *Diabetes*, *58*(7), 1526–1531.

Schneider, D. L., Barrett-Connor, E. L., & Morton, D. J. (1994). Thyroid hormone use and bone mineral density in elderly women. Effects of estrogen. *JAMA: the journal of the American Medical Association*, *271*(16), 1245–1,249.

Schneider, D. L., Barrett-Connor, E. L., & Morton, D. J. (1995). Thyroid hormone use and bone mineral density in elderly men. *Archives of Internal Medicine*, *155*(18), 2005–2007.

Serrat, M. A. (2013). Allen's rule revisited: Temperature influences bone elongation during a critical period of postnatal development. *The Anatomical Record*, *296*(10), 1534–1,545.

Serrat, M. A. (2014). Environmental temperature impact on bone and cartilage growth. *Comprehensive Physiology*, *4*(2), 621–655.

Serrat, M. A., King, D., & Lovejoy, C. O. (2008). Temperature regulates limb length in homeotherms by directly modulating cartilage growth. *Proceedings of the National Academy of Sciences of the United States of America*, *105*(49), 19348–19353.

Serrat, M. A., Schlierf, T. J., Efaw, M. L., Shuler, F. D., Godby, J., Stanko, L. M., & Tamski, H. L. (2015). Unilateral heat accelerates bone elongation and lengthens extremities of growing mice. *Journal of Orthopaedic Research*, *33*(5), 692–698.

Serrat, M. A., Williams, R. M., & Farnum, C. E. (2009). Temperature alters solute transport in growth plate cartilage measured by in vivo multiphoton microscopy. *Journal of Applied Physiology*, *106*(6), 2016–2025.

Serrat, M. A., Williams, R. M., & Farnum, C. E. (2010). Exercise mitigates the stunting effect of cold temperature on limb elongation in mice by increasing solute delivery to the growth plate. *Journal of Applied Physiology*, *109*(6), 1869–1879.

Sharp, L. Z., Shinoda, K., Ohno, H., Scheel, D. W., Tomoda, E., Ruiz, L., et al. (2012). Human BAT possesses molecular signatures that resemble beige/brite cells. *PLoS One*, *7*(11), e49452.

Sinder, B. P., Salemi, J. D., Ominsky, M. S., Caird, M. S., Marini, J. C., & Kozloff, K. M. (2015). Rapidly growing Brtl/+ mouse model of osteogenesis imperfecta improves bone mass and strength with sclerostin antibody treatment. *Bone*, *71*, 115–123.

Smith, L., Bigelow, E. M., & Jepsen, K. J. (2013). Systematic evaluation of skeletal mechanical function. *Current Protocols in Mouse Biology*, *3*, 39–67.

Speakman, J. R., & Keijer, J. (2012). Not so hot: Optimal housing temperatures for mice to mimic the thermal environment of humans. *Molecular Metabolism*, *2*(1), 5–9.

Steegmann, A. T., Jr. (2007). Human cold adaptation: An unfinished agenda. *American Journal of Human Biology: The Official Journal of the Human Biology Council*, *19*(2), 218–227.

Sumner, F. B. (1909). Some effects of external conditions upon the white mouse. *Journal of Experimental Zoology*, *7*(1), 97–155.

Thompson, D. D., & Gunness-Hey, M. (1981). Bone mineral-osteon analysis of Yupik-Inupiaq skeletons. *American Journal of Physical Anthropology*, *55*(1), 1–7.

Toth, L. A., Trammell, R. A., & Ilsley-Woods, M. (2015). Interactions between housing density and ambient temperature in the cage environment: Effects on mouse physiology and behavior. *Journal of the American Association for Laboratory Animal Science*, *54*(6), 708–717.

van Marken Lichtenbelt, W. D., Vanhommerig, J. W., Smulders, N. M., Drossaerts, J. M., Kemerink, G. J., Bouvy, N. D., … Teule, G. J. (2009). Cold-activated brown adipose tissue in healthy men. *The New England Journal of Medicine*, *360*(15), 1500–1508.

Virtanen, K. A., Lidell, M. E., Orava, J., Heglind, M., Westergren, R., Niemi, T., et al. (2009). Functional brown adipose tissue in healthy adults. *The New England Journal of Medicine*, *360*(15), 1518–1525.

Wallace, I. J., Nesbitt, A., Mongle, C., Gould, E. S., & Grine, F. E. (2014). Age-related variation in limb bone diaphyseal structure among Inuit foragers from point hope, northern Alaska. *Archives of Osteoporosis*, *9*, 202.

Weaver, M. E., & Ingram, D. L. (1969). Morphological changes in swine associated with environmental temperature. *Ecology*, *50*(4), 710–713.

Wu J, Bostrom P, Sparks LM, Ye L, Choi JH, Giang AH, Khandekar M, Virtanen KA, Nuutila P, Schaart G Spiegelman BM 2012. Beige adipocytes are a distinct type of thermogenic fat cell in mouse and human. *Cell 150*(2):366–376.

Yang, S., Nguyen, N. D., Eisman, J. A., & Nguyen, T. V. (2012). Association between beta-blockers and fracture risk: A Bayesian meta-analysis. *Bone*, *51*(5), 969–974.

How to cite this article: Robbins A, Tom Christina A. T. M. B., Cosman MN, et al. Low temperature decreases bone mass in mice: Implications for humans. *Am J Phys Anthropol*. 2018; 167:557–568. https://doi.org/10.1002/ajpa.23684